

Supplementary Material for

Mechanism of ice nucleation in liquid water on alkali feldspars

Alice Keinert^a, Kathrin Deck^{b,*}, Tilia Gädecke^a, Thomas Leisner^{a,c} and Alexei A. Kiselev^{a,*}

^a Karlsruhe Institute of Technology, Institute of Meteorology and Climate Research, Karlsruhe, Germany

^b Now at TU Delft, Faculty of Aerospace Engineering, Department of control and operations, Delft, The Netherlands

^c Institut für Umweltphysik, Universität Heidelberg, Heidelberg, Germany

* Correspondence should be addressed to alexei.kiselev@kit.edu

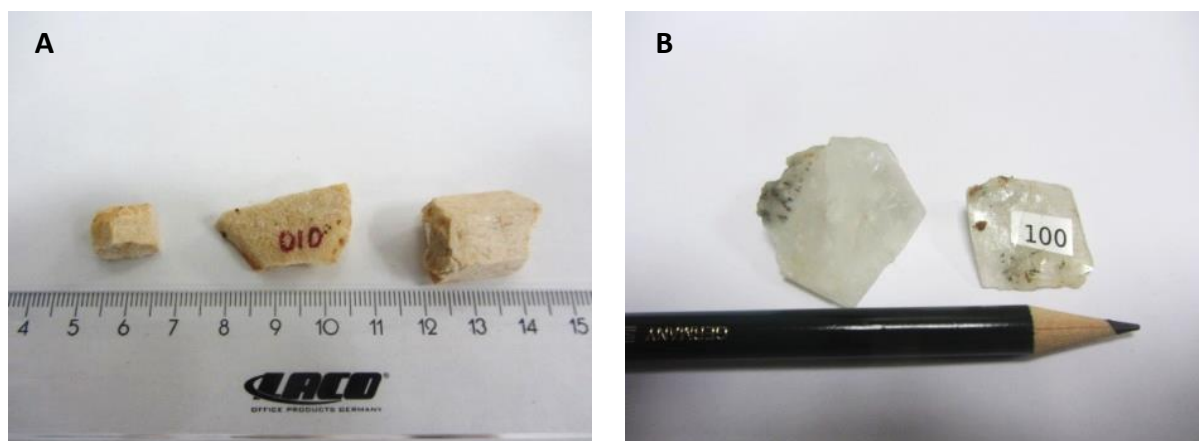


Figure S1. Feldspar specimens used for preparation of thin sections and powder samples in this study.

A. Microcline feldspar from Pakistan (FS06). **B.** Adularia sanidine feldspar (FS07).

The cleavage planes (001) and (010) were initially identified from the specimen appearance and angular relationships between the free growing planes and confirmed by back-scattered electron diffractometry (BSED).

Table ST1. Lattice constants and fractional composition of feldspar specimens FS06 and FS07 determined for powder samples with XRD (Panalytical, Cu K-alpha 1&2), courtesy of Jörg Göttlicher, (IPS, KIT)

Lattice constants	FS06			FS07
	orthoclase	microcline	albite	orthoclase
a [Å]	8.58499(28)	8.59735(55)	8.14127(51)	8.55046(96)
b [Å]	12.98310(27)	12.97389(87)	12.7979(12)	12.9762(12)
c [Å]	7.20553(16)	7.21518(54)	7.15525(60)	7.20556(47)
α [°]	90	90.2851(84)	94.251(12)	90
β [°]	116.0177(22)	116.0222(65)	116.5891(74)	116.0151(75)
γ [°]	90	88.9051(72)	87.8129(94)	90
Volume [Å ³]	721.736(35)	723.066(95)	664.82(10)	718.47(12)
Fraction [%]	41.08	39.51	19.40	90.44

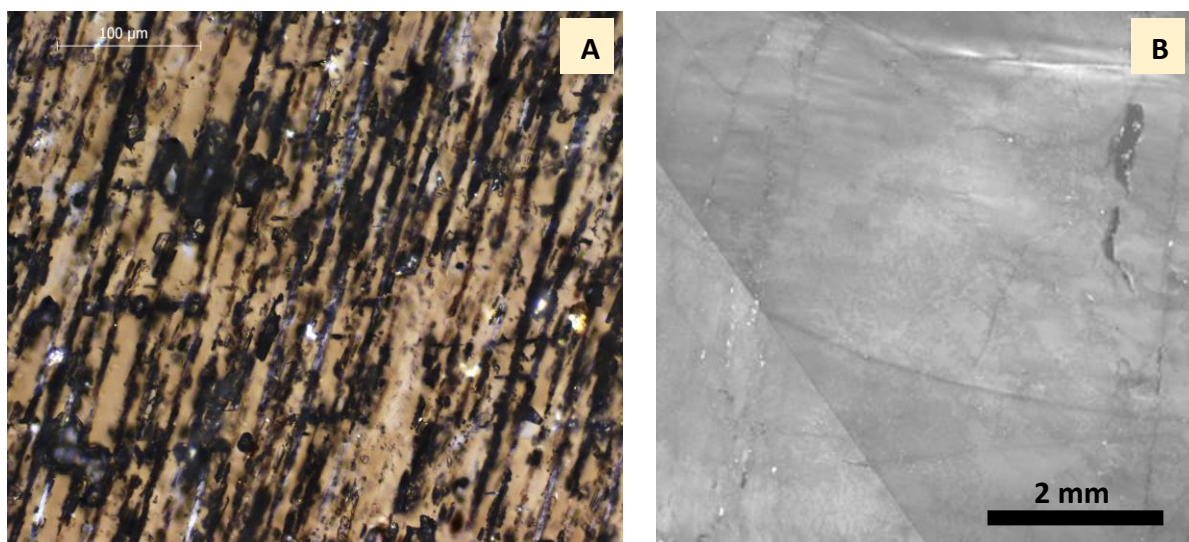


Figure S2. Polarization microscope images the petrographic thin sections of feldspar (with thickness appr. 20 μm). **A.** Microcline feldspar FS06 thin section with Miller index (010) exhibits fully coherent film lamellae (alternating dark and light beige stripes). **B.** Adularia sanidine feldspar (Sample FS07) section prepared along (010) is free of microtexture. The oblique line in the left bottom quarter of the image in panel B is the twin boundary.

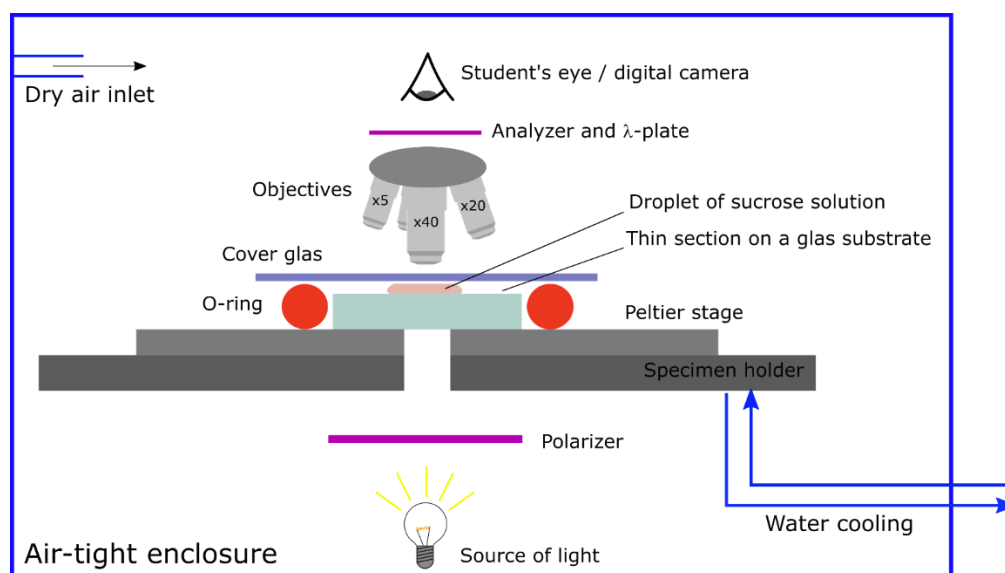


Figure S3. Experimental setup for studying ice nucleation and growth in sucrose solution. A small droplet (approximately 1 μL volume) of 60 wt% aqueous solution of sucrose (Merk) was placed on the surface of a sample thin section and covered with microscope cover slide to avoid evaporation. The sample (thin section on a glass slide) was positioned on the Peltier stage mounted on the rotation table of the polarization microscope (Leica DM4), and the whole microscope was enclosed into an air-tight flexible glove box filled with water-free synthetic air to avoid water condensation and frost formation on the cold surfaces. The Peltier stage was slowly cooled down to -30°C or until several ice crystals became visible in the field of view of the microscope. The temperature was then manually adjusted to the apparent melting point of ice in the sucrose solution (between -13°C and -15°C) to slow down or completely stop the growth of ice crystals.

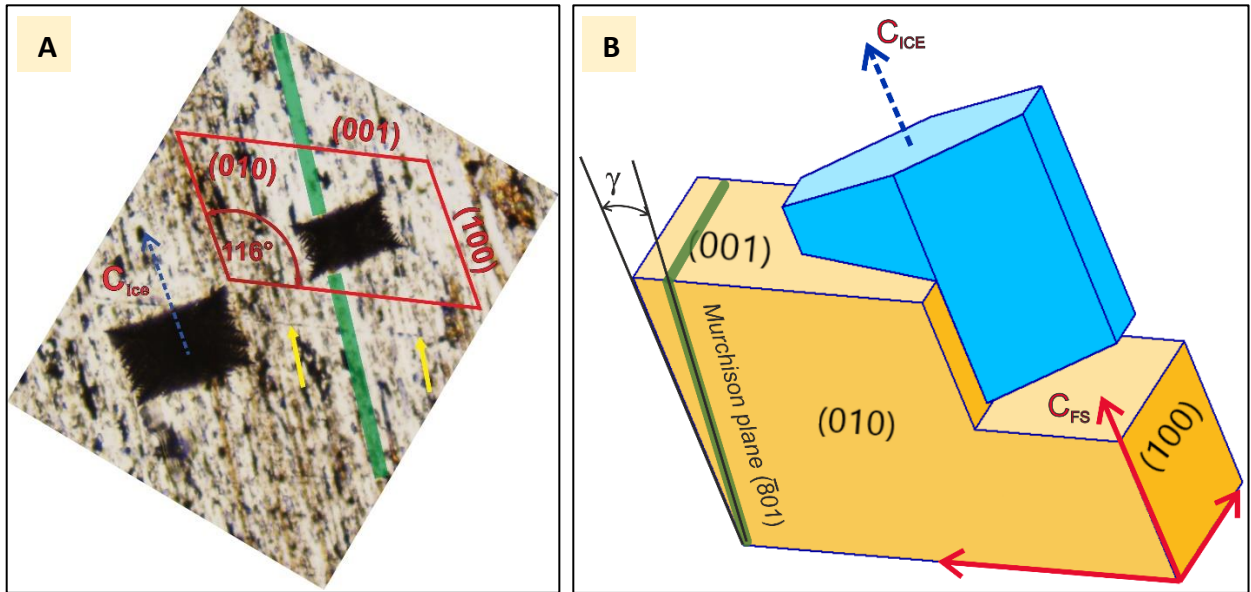


Figure S4. Relative orientation of ice and the FS06 feldspar crystalline lattice. **A.** The ice crystals (dark rectangles) growing upon the FS06 (010) thin section as seen in a polarization microscope, overlaid with the projection of feldspar lattice unit cell (in red) and projection of the Murchison ($\bar{8}01$) plane (the green band). The Murchison plane is inclined by an angle $\gamma \in [8^\circ, 11^\circ]$ to the (100) plane. The yellow arrows indicate the position of the cleavage plane (001) orthogonal to the plane of image. The background image is rotated to match the orientation of the (010) face of feldspar in the panel (B). **B.** Primitive unit of microcline feldspar with an ice crystal epitaxially grown on the (100) plane. The lines formed by the Murchison plane crossing (010) and (001) are shown in green.

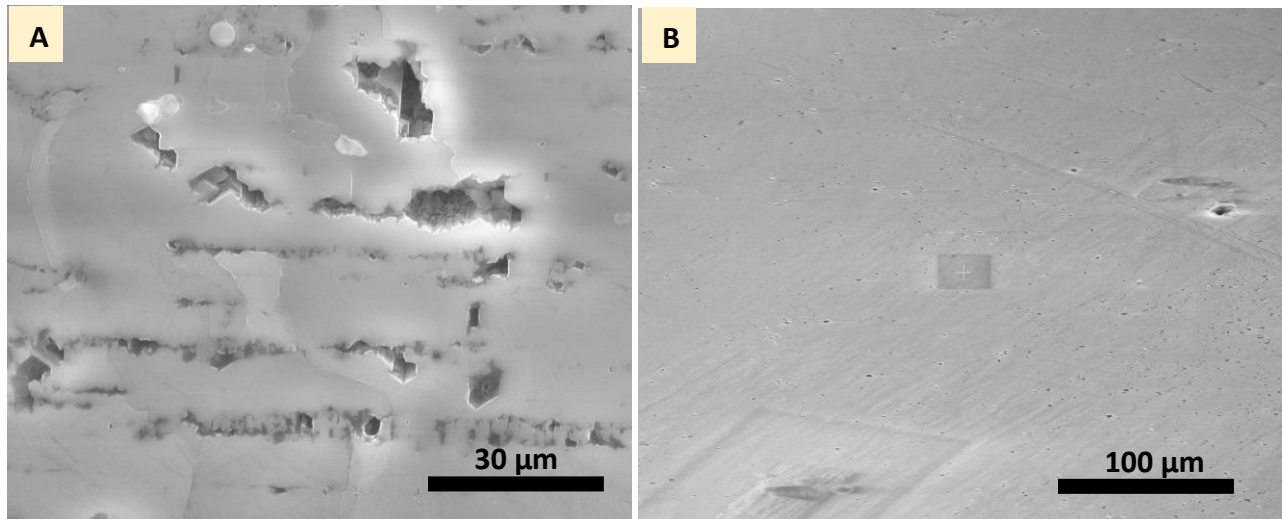


Figure S5. ESEM images of the thin sections of feldspar specimens FS06 and FS07. **A.** A close-up image of the FS06 (010) thin section surface showing multiple cavities and pits aligned with the borders of the perthitic

exsolution lamellae. **B.** The surface of the FS07 (010) polished thin section viewed at 60° angle appears smooth apart from several scratches and occasional surface defects (dark dots).

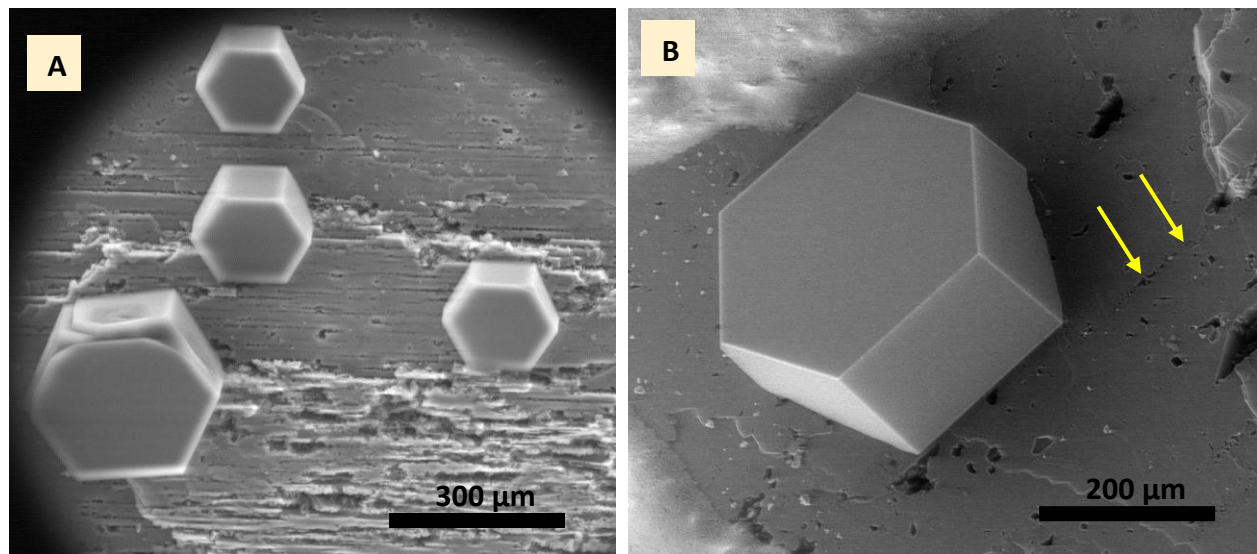


Figure S6. ESEM image of ice on cleaved (but not polished!) FS06 (001) surface. Feldspar sample was cooled down to -28°C to achieve ice nucleation and growth. The overall pressure in the specimen chamber was 450 Pa (humidified N₂ gas) and the partial water pressure about 50 Pa, which is below the water saturation but above the ice saturation pressure at this temperature. **A.** Orientation of ice crystals with the prism face parallel to the cracks and tilt to the surface (expected to be equal 26°) imply an epitaxial growth of ice on the (100) surface. **B.** The arrows show the pits in the surface aligned with the boarder of an exsolution lamella.

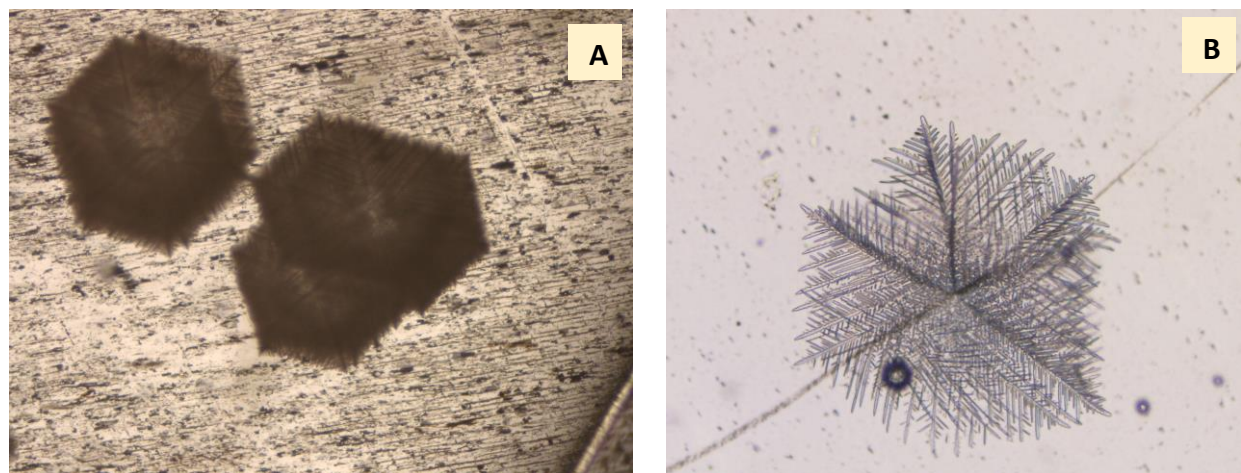


Figure S7. Ice crystals growing in sucrose solution on top of the thin sections of feldspar specimens. **A.** Thin section prepared along the (001) surface of FS06 specimen. The 5 ice crystals are the only 5 crystals that showed oriented growth on this surface, but their orientation could not be reliably used to determine the relationship between the crystalline structures of ice and feldspar. **B.** A “thinned” ice crystal nucleating at the crack in the FS07 (001) surface.